

Steady and Unsteady calculations on Thermal Striping Phenomena in Triple-Parallel Jet

Y.Q. Yu¹, E. Merzari¹, J.W.Thomas¹, A. Obabko²

¹: Nuclear Engineering Division, Argonne National laboratory, Lemont, IL 60439, United State

²: Mathematics and Computer Science Division, Argonne National laboratory, Lemont, IL
60439, United State

yyu@anl.gov

Abstract

The particular phenomena of thermal striping are encountered in liquid metal cooled fast reactors (LMFR), in which temperature fluctuation due to convective mixing between hot and cold fluids can lead to a possibility of crack initiation and propagation in the structure due to high cycle thermal fatigue. Using sodium experiments of parallel triple jets configuration performed by Japan Atomic Energy Agency (JAEA) as benchmark, numerical simulations were carried out to evaluate the temperature fluctuation characteristics in fluid and the transfer characteristics of temperature fluctuation from fluid to structure, which is important to assess the potential thermal fatigue damage. In this study, both steady (RANS) and unsteady (URANS, LES) calculations were applied to predict the temperature fluctuations of thermal striping. The verifications on mesh density and boundary conditions were carried out. The velocity, temperature and temperature fluctuation intensity distribution were compared with the experimental data. The steady calculation has limited success in predicting the thermal hydraulic characteristics of the thermal striping, highlighting the limitations of the RANS approach in unsteady heat transfer simulations. The unsteady results exhibited reasonably good agreement with experimental results for temperature fluctuation intensity, as well as the average temperature and velocity components at the measurement locations.

Keywords: thermal striping, triple jets, URANS, LES

1. Introduction

Fluctuating temperatures in the core outlet of sodium-cooled fast reactors (SFRs) may cause high-cycle thermal fatigue (a.k.a. thermal striping) in the structures in the upper plenum, eventually causing damage to important structures above the core. Jets expel from each of the core subassemblies into the outlet plenum (or hot pool), and the mixing from interacting, turbulent jets of a wide range of flow rates and temperatures results in highly complex flow and temperature evolutions. Nearby structures, including core instrumentation, control rod drivelines, and their supports, may see a range fluctuating fluid temperatures during normal operation. Predicting this phenomenon, which is important for design and operation, is further complicated by the influence of the solid structure on the fluid temperature caused by the difference in heat capacity. Such code predictions need to be validated against relevant experiments before they can be trusted in design studies or supporting safety and licensing activities. Experiments using sodium are particularly useful, because its high thermal conductivity influences the time-scale of these fluctuations. Unfortunately, because sodium is opaque, simultaneous optical techniques of measuring high-resolution velocity profiles in sodium are not possible. Therefore, validating the velocity predictions must utilize experiments in transparent fluids like water and air.

The problem of thermal striping in the core outlet region of SFRs is of great interest to the international community. The JAEA cites early work by Wood [1] and Brunings [2], Betts [3], Moriya [4] and Tokuhiko [5] in their reports, and the CEA's Tenchine [6, 7] investigated the mixing behavior of co-axial jets of sodium and compared the results of sodium with air jets experiment. In the DOE complex, the most recent experiments have been performed using Argonne's coaxial air-jet mixing facility MAX, which employs the high-resolution optical measurement techniques for the velocity distribution, along with wall surface temperature measurements via thermal imaging and within-jet temperature profile measurements via fiber optics [8, 9].

Because of the importance of validating thermal striping predictions to the international community, and the value of high-quality measurements of the phenomenon in sodium, the members STC-A7 collaboration on Sodium-Cooled Fast Reactor Thermal-Hydraulics decided to initiate a benchmark exercise using the JAEA experiment PLAJECT, which is part of a larger series of related experiments in turbulent jet mixing. Tokuhiko [10, 11] and Kimura [12, 13] performed a water experiment of the triple-parallel jets mixing phenomena called WAJECO and evaluated the mixing process among the jets. The attenuation process of the temperature fluctuation from fluid to structure was very important to predict the thermal striping phenomena. Kimura [14] performed a sodium experiment called as PLAJECT that had triple-parallel jets along a stainless steel wall and showed that the transfer characteristics of temperature fluctuation from fluid to structure could be evaluated by using a heat transfer coefficient obtained from a transfer function between temperature fluctuations in fluid and structure. Furthermore, in the water experiment WAJECO with the same configured test section in the sodium experiment PLAJECT, a stainless steel plate with thermocouples was set along flow in order to evaluate the characteristics of temperature fluctuation transfer from fluid to structure compared with that in the sodium experiment [15, 16].

This paper provides a description of the PLAJECT benchmark problem. Furthermore, both steady (RANS) and unsteady (URANS, LES) calculations were applied to predict the thermal striping. The benchmark exercise in this paper is being performed under the auspices of an international collaboration on thermal hydraulics for sodium-cooled fast reactor development

with participation from the Japan Atomic Energy Agency, the U.S. Department of Energy, and the France's Commissariat a l'energie atomique et aux energies alternatives.

2. Description of PLAJECT Experiment and Benchmark specifications

Figure 3-1 shows a schematic of the test section of PLAJECT. The x -axis corresponds to the depth direction normal to the vertical wall, the y -axis is horizontal direction in which the jets are aligned, and the z -axis is vertical direction in which flow is injected. The origin is set at the center of the cold jet on the nozzle outlet and on the wall surface. In the test section, a rectangular metal block with slope on both sides is installed in the bottom of the test section. The metal block has three discharged nozzle outlets on the top surface. The height of the block is 85 mm from the bottom of the test section. The cross section of each nozzle outlet is rectangular. Width in the horizontal direction is 20 mm and nozzle length in depth direction is 180 mm. A cold jet vertically flows out from the center nozzle and the hot jets vertically flow out from the nozzle outlets on both sides of the center. The test section is placed between two vertical plates. The parallel plates are installed on both sides in depth direction of the nozzle block. One of the SS316 plates is instrumented to investigate temperature fluctuation in the structure.

Table 2-1 shows typical experimental conditions as candidates for the benchmark exercise. The Reynolds number is defined as follows:

$$Re = \frac{V_m D}{\nu} \quad (2-1)$$

$$V_m = \frac{V_c + 2V_h}{3} \quad (2-2)$$

D is a nozzle width (=20 mm) and V_m is mean discharged velocity of three jets. V_c is the mean velocity of the cold jet from the center nozzle and V_h is the mean velocity of the hot jets from the nozzles on both sides. The discharged temperature difference, ΔT , is defined as follows:

$$\Delta T = T_h - T_c \quad (2-3)$$

T_h and T_c are time-averaged temperatures at the nozzle of the hot and cold jet respectively. Since the temperature difference is not so large, dependency of thermal property is not considered in the estimation of mixed-mean temperature T_m as:

$$T_m = \frac{V_c T_c + 2V_h T_h}{3V_m} \quad (2-4)$$

Table 2-1 Experimental Conditions

Case	Outer-slits/Hot Jets		Center-slit/Cold Jet		Mixture		
	V_h (m/s)	T_h (°C)	V_c (m/s)	T_c (°C)	V_m (m/s)	ΔT (°C)	T_m (°C)
A1	0.51	347.5	0.51	304.5	0.51	43	333.2
A2	0.48	40.3	0.48	32.0	0.48	8.3	37.5
B1	0.51	349.8	0.32	311.0	0.45	38.8	340.5

The iso-velocity case (Case A1) in which a characteristic dominant frequency was observed in the fluid temperature fluctuation around the center jet in the mixing region with stainless steel plate are selected as a candidate in benchmark exercise.

3. Numerical Methodology

3.1 Computational Domain and Mesh Generation

Figure 3-1 shows the computational domain of 198 mm (=180mm+18mm) in depth, 500 mm in horizontal direction and 685 mm (=600mm + 85mm) in vertical direction from the bottom of the test section. Figure 3-1 also provides a numbering scheme for the outer boundaries, which will be referenced in the description of the boundary condition sensitivity studies. The figure also indicates a smaller region used to visualize the results. This domain is enlarged three times in horizontal direction for boundary condition choosing purpose, which is further discussed in section 3.2.

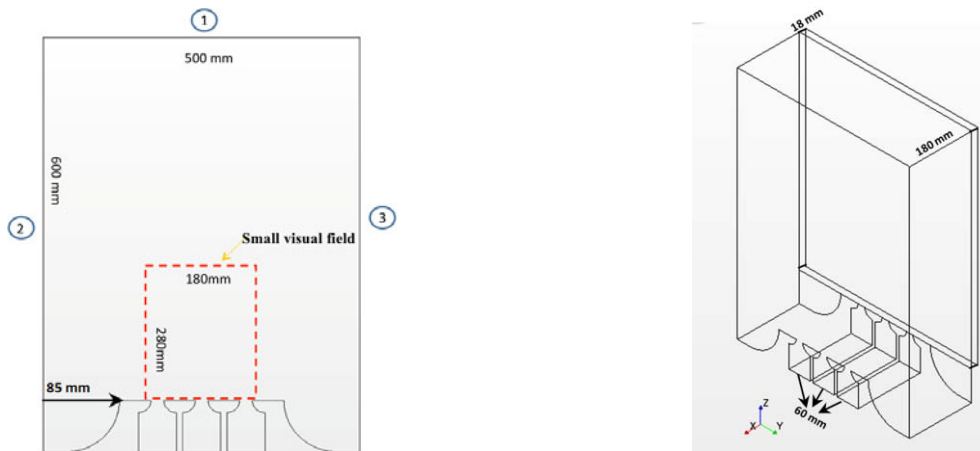


Figure 3-1. Computational Domain for the Model of the PLAJECT Benchmark

Two planes and two lines in the computational domain are identified where code predictions for the velocity and temperature distribution have been extracted in later plots. They are referenced as the center plane, the near-wall plane, the centerline and the near-wall line in the following content. The center plane ($x=85\text{mm}$) is in the middle of two partition plates and the near-wall plane ($x=1\text{mm}$) is in the vicinity of one partition plate. The two lines are on the two planes respectively at $z=100\text{mm}$ from the nozzle exit in the vertical position where the main convective mixing occurred. All the velocity components are normalized with the discharged velocity $V_{exit}=0.51\text{m/s}$. The temperature is normalized by the following equation:

$$T^* = \frac{(T - T_c)}{\Delta T} \quad (3-1)$$

where T^* is non-dimensional temperature, ΔT is the temperature difference between hot jet and cold jet.

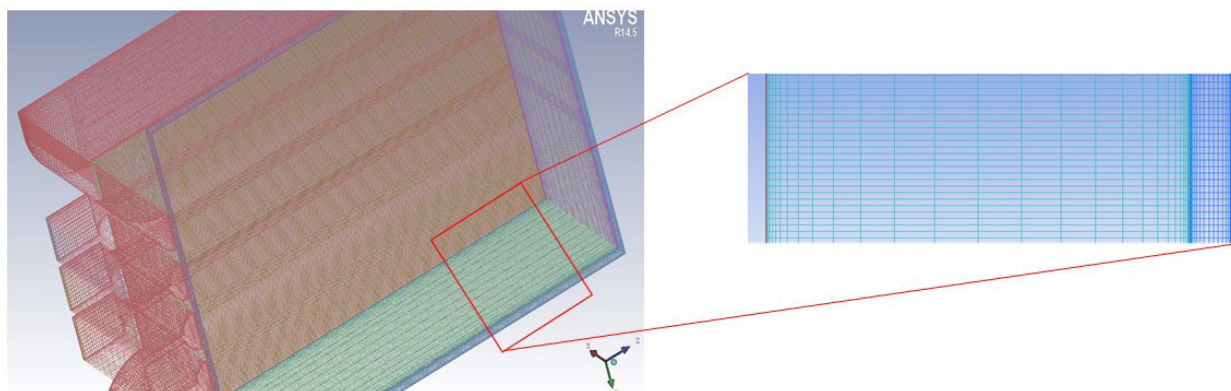


Figure 3-2. Hexahedral Mesh Structure

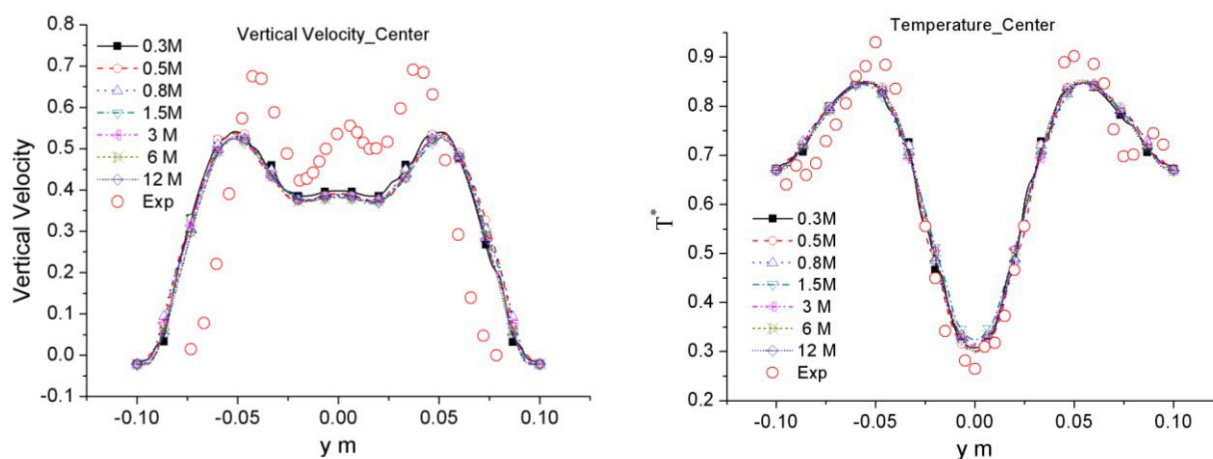


Figure 3-3. Results of mesh refinement study: velocity (left) and temperature(right) profiles at $z=100\text{mm}$ above jets

The purely hexahedral mesh (Figure 3-2) is employed in this benchmark study. A mesh sensitivity study is performed guaranteeing y^+ at the wall below 1. The cell number of the meshes ranges from 0.3 million to 12 million. The Effect of the number of cells on the velocity and temperature distribution is shown in Figure 3-3. No remarkable effect is observed. In order to obtain a reasonable resolution of the simulation, mesh of 3 million cell is chosen for RANS analysis. A refined mesh was generated for the URANS and LES analysis, primarily motivated by the mesh requirements for LES. A detailed description of the mesh is listed in Table 3-1.

Table 3-1. STAR-CCM+ Mesh Description

		Horizontal	Normal Direction to wall	Vertical
Coarse Mesh for steady-state RANS				
Fluid	Number of Mesh	250	35	330
	Minimum of Mesh Size	2 mm	0.08 mm	2 mm

Refined Mesh for URANS and LES				
Fluid	Number of Mesh	364	55	393
	Minimum of Mesh Size	2 mm	0.08 mm	2 mm
Structure	Number of Mesh	364	38	343
	Minimum of Mesh Size	2 mm	0.05 mm	2 mm

3.2 Boundary Conditions

A sensitivity study was performed to investigate the influence of various boundary condition options. In this study, steady-state RANS simulations were performed, and the solid walls were not considered. The boundary conditions applied to the three boundaries are labeled symmetry (S), outlet (O), flow-split (F), and periodic (P), according to the ordering indicated in Figure 3-1.

Since it's hard to determine the fraction of the flow exit from the side boundary experimentally, a simulation with three times wider computational domain in horizontal direction was performed to provide a reference data. The deviations of the flow fraction exit from the side boundary by using various boundary conditions are listed in Table 3-2.

Table 3-2. Flow fraction exit from the side boundary

	FOO	FPP	FSS	OSS	OPP	OOO	Reference
Fraction	6.5%	10.4%	0	0	52.1%	31.3%	25.8%
Deviation	19.3%	15.4%	25.8%	25.8%	-26.3%	-5.5%	0

Some velocity vectors on the center plane are shown in Figure 3-4, which may help us have a better understanding on the effect of the boundary condition. In general, the effect of the boundary condition on the flow field in the small visual field is negligible since the boundary of the whole computational domain is sufficiently far from the small visual field. However, the boundary condition does have obvious effect on flow distribution outside the small visual field, especially in the region near the boundary. In FOO case, most flow exits from the top; only a small amount of fluid exit from the sides. In FSS case, two symmetric vortexes appear on both side of the main stream, no flow exit or enter the domain from the sides due to the symmetry boundary condition. In OOO case, flow exit from the top and the sides evenly with no vortex observed. After all, symmetry boundary condition is not recommended if the computational cost is affordable because it adds some restrains on the flow near the boundary and may cause artificial recirculation of the flow. Based on the quantitative analysis, OOO is taken as the best combination. This boundary condition option was also applied to the URANS and LES analysis.

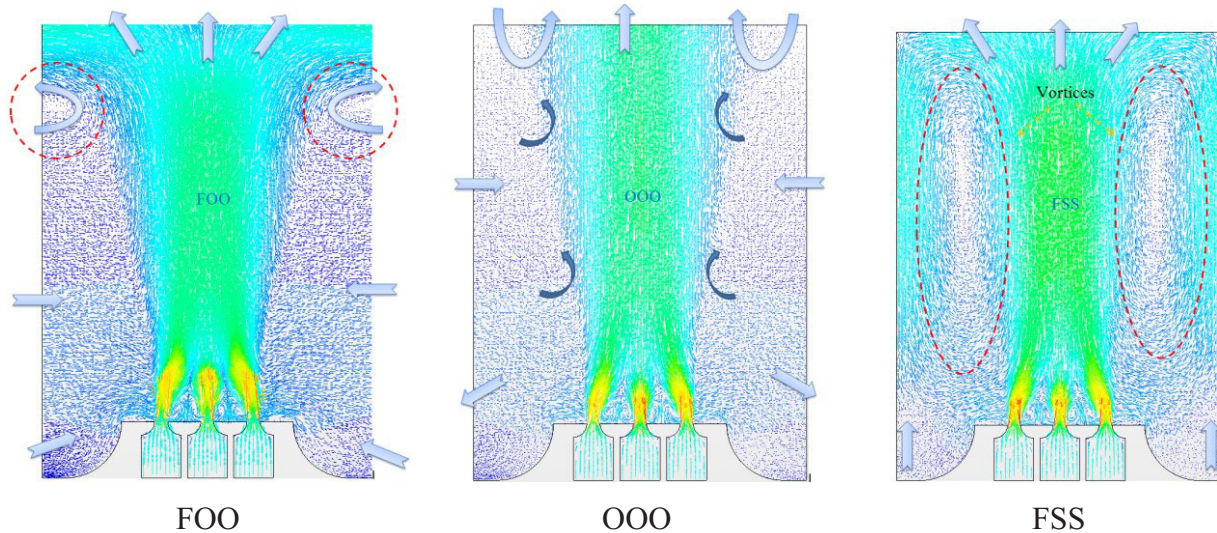


Figure 3-4. Velocity Vector on the Center Plane

4. Results and Discussions

4.1 Instantaneous Quantities

The velocity and temperature fluctuations predicted with URANS model are presented in Figure 4-1. The velocity ranges from 0.14m/s to 0.36m/s while temperature ranges from 311°C to 343°C. Figure 4-2 shows the instant temperature fluctuation in a vivid way. The hot jets on both sides periodically lean to the cold jet, which results in the formation of some low temperature region. With the movement of these cold regions, the heat transfer between the fluids within these cold regions and the ambient hot fluid occur.

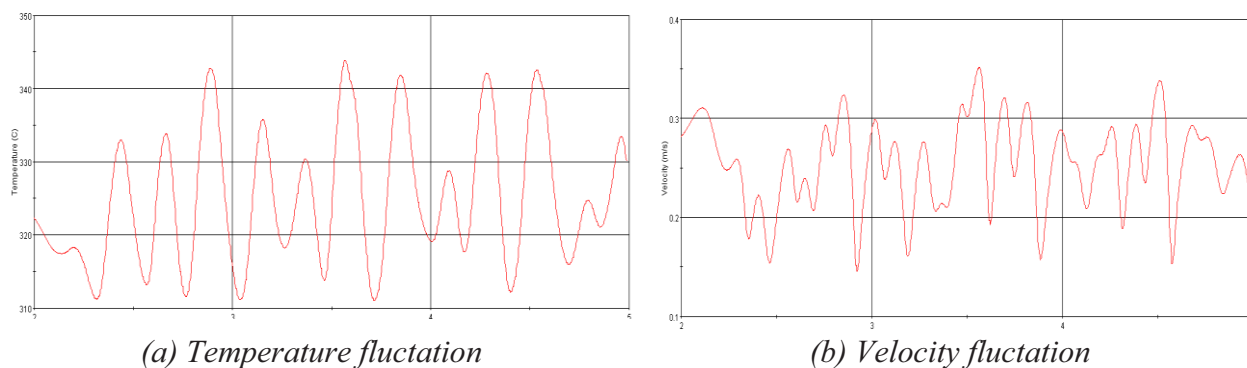


Figure 4-1. Temperature and Velocity fluctuation in URANS model

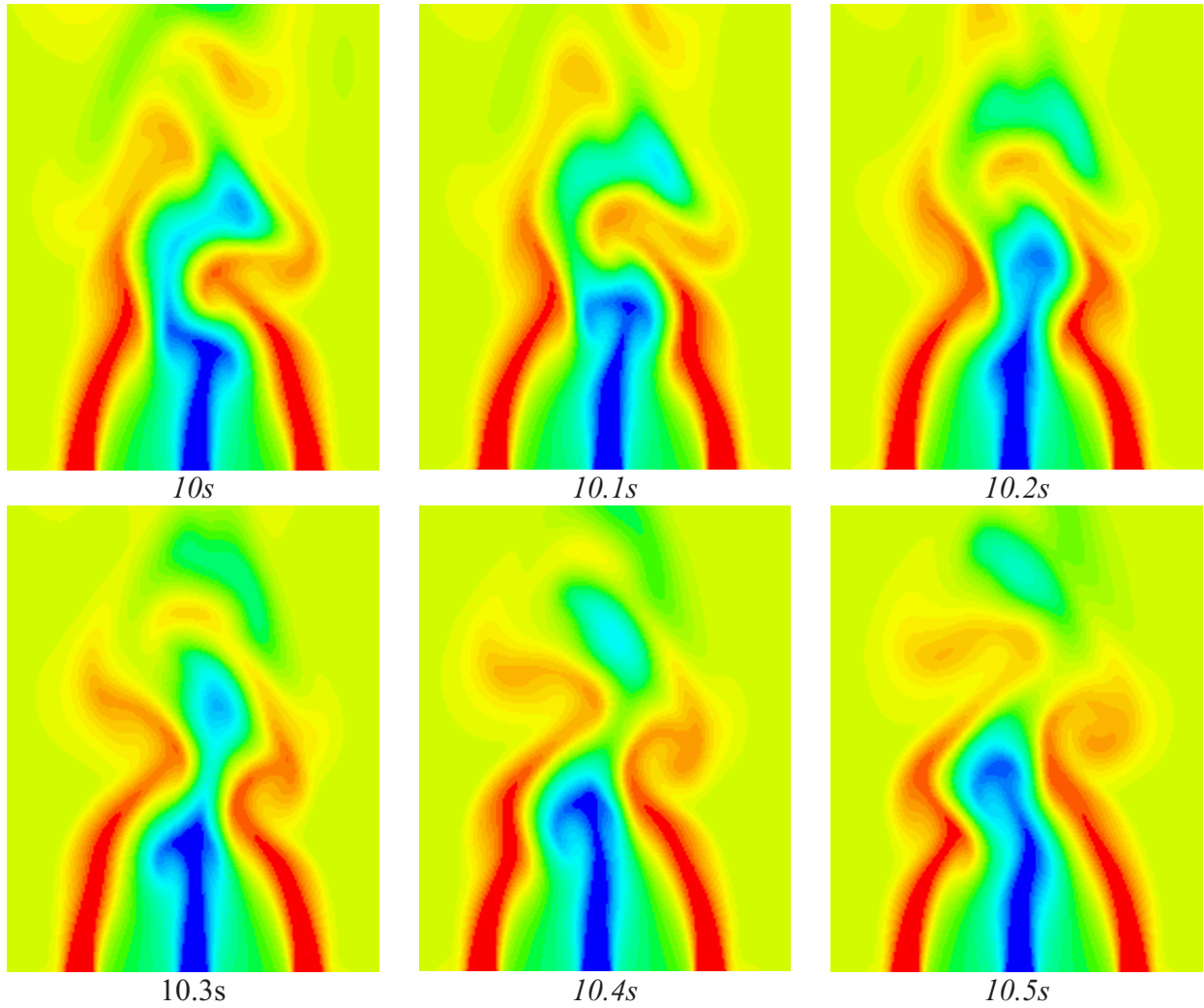


Figure 4-2. Temperature Contour on the Center Plane at Different Time Instance

4.2 Time Mean Quantities

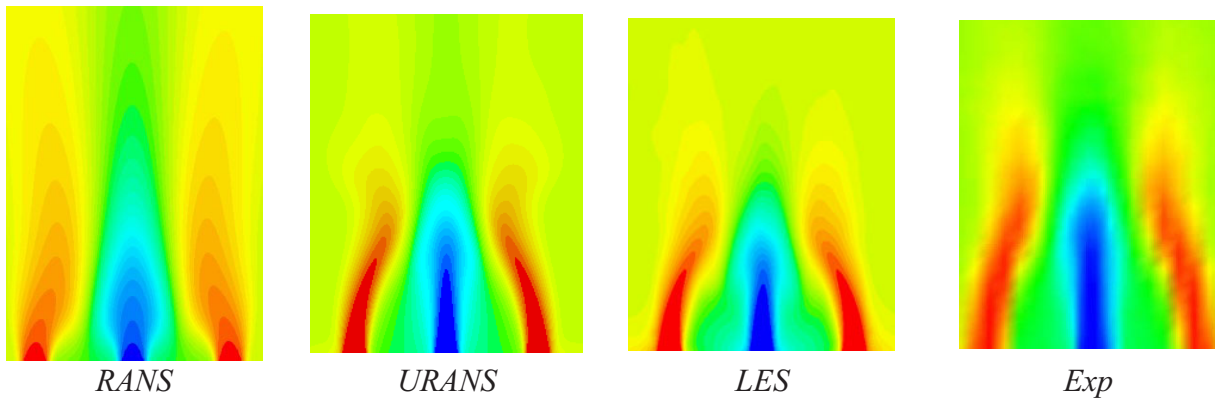


Figure 4-3. Time-averaged Temperature Contour on the Center Plane

Figure 4-3 presents the time-averaged temperature distribution on the center plane with RANS, URANS and LES model. The shapes of the cold region (in blue) and the hot region (in red) with both URANS and LES model achieve good agreements with the experiment.

In Figure 4-4, a comparison of the time-averaged temperature fluctuation intensity (TFI) on the center plane between URANS, LES and experiment was shown. Temperature fluctuation intensity, TFI, is defined as a standard deviation of temperature as follows:

$$TFI = \sqrt{\frac{1}{N} \sum_{i=1}^N (T_i - T_{avg})^2} \quad (4-1)$$

Moreover, the normalized temperature fluctuation intensity is as follows:

$$TFI^* = \frac{TFI}{\Delta T} \quad (4-2)$$

The contour pattern looks like a “butterfly”, which agrees well with the experiment. Both URANS and LES model overestimate the TFI at $z=80\sim 120\text{mm}$ vertically and in the region between the hot and the cold jst horizontally.

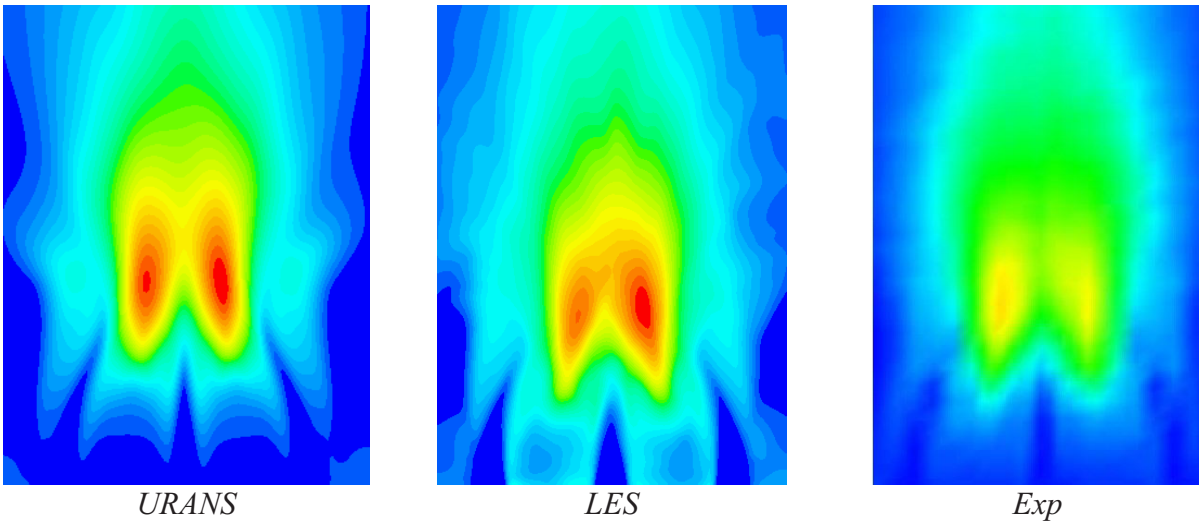
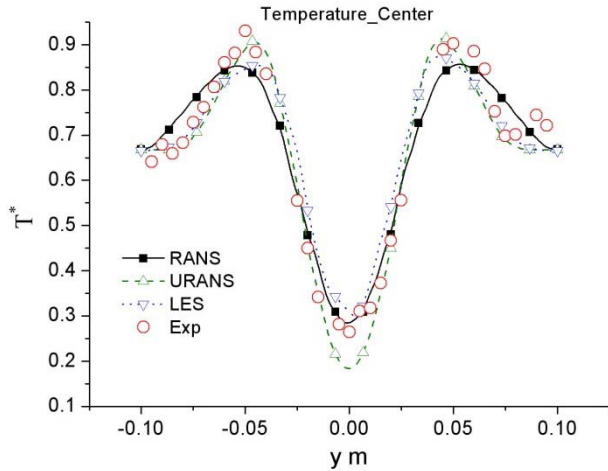


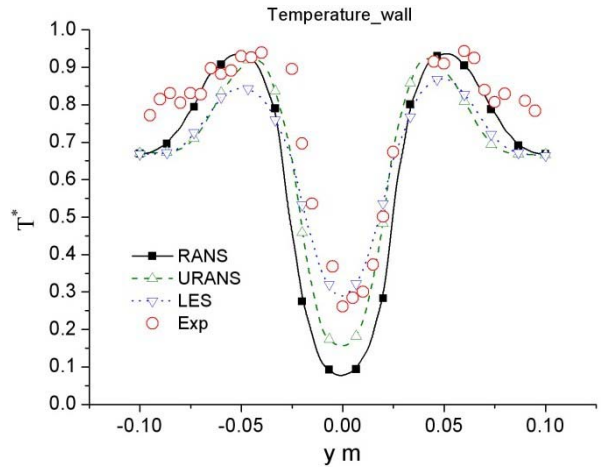
Figure 4-4. Contour of Temperature Fluctuation Intensity on the Center Plane

Figure 4-5 shows the comparison of the temperature distribution, velocity component and temperature fluctuation intensity on the centerline and the near-wall line between RANS, URANS and LES models. The remarkable improvements on the prediction are achieved with URANS and LES model. The LES model predicts the experiment better than the URANS model does, especially on the TFI near the wall, which is significant to evaluate the thermal fatigue.

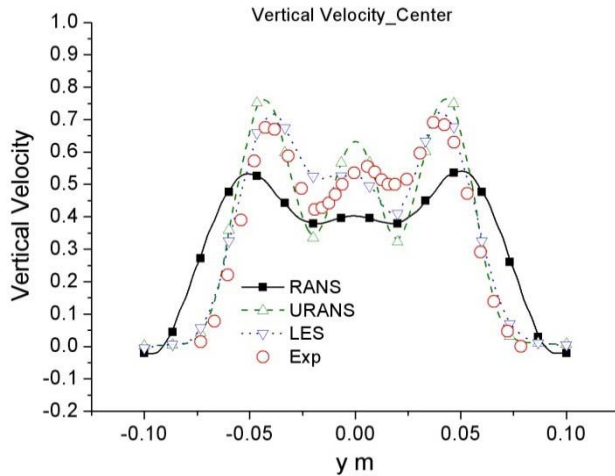
Figure 4-6 shows the temperature fluctuation intensity distribution in normal direction to wall surface. The decay of the TFI in structure is in good agreement with the experiment. It seems that the LES model with conjugate heat transfer can model the thermal interaction between the fluid and the structure well.



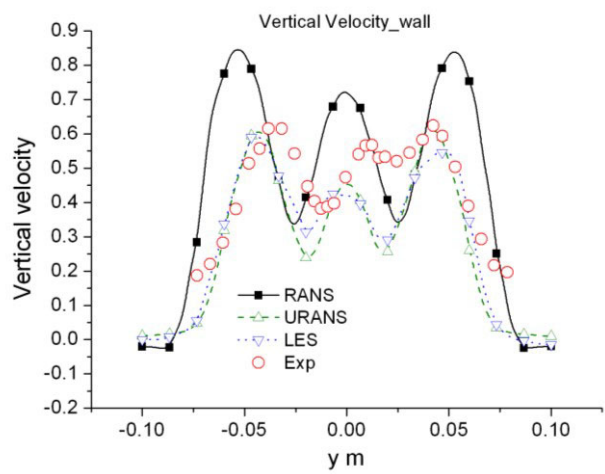
(a) Temperature along the centerline



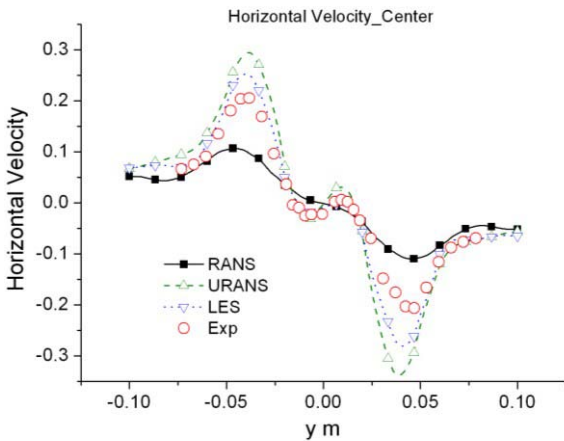
(b) Temperature along the near-wall line



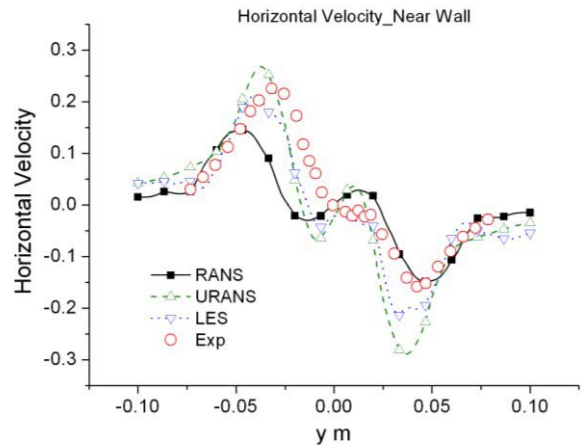
(c) Vertical Velocity along the centerline



(d) Vertical Velocity along the near-wall line



(e) Horizontal Velocity along the centerline



(f) Horizontal Velocity along the near-wall line

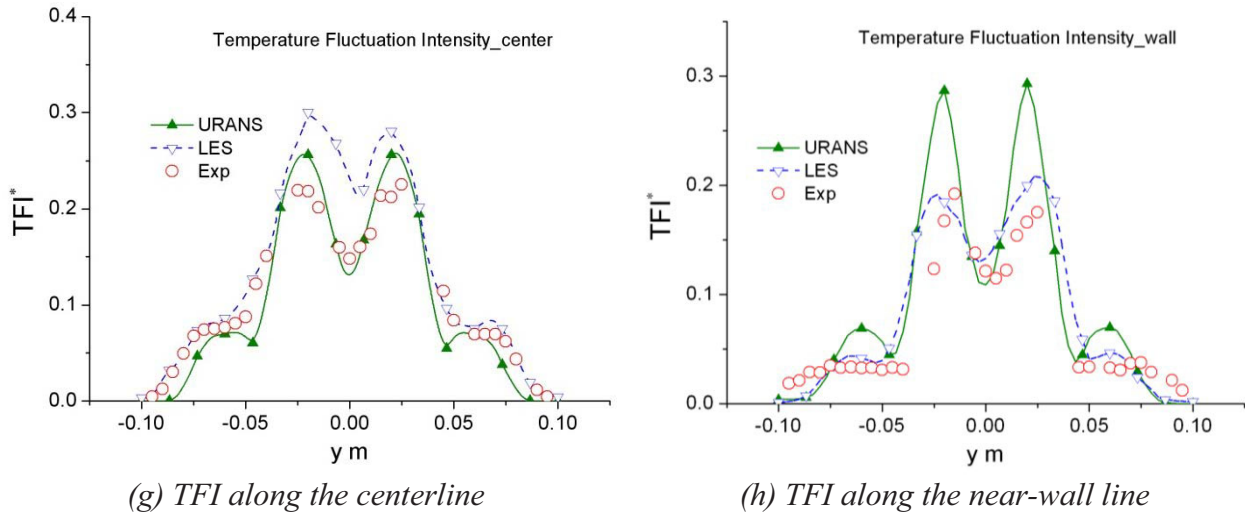


Figure 4-5. Temperature, Velocity component and Temperature Fluctuation Intensity on the Centerline and the near-wall with RANS, URANS and LES Models

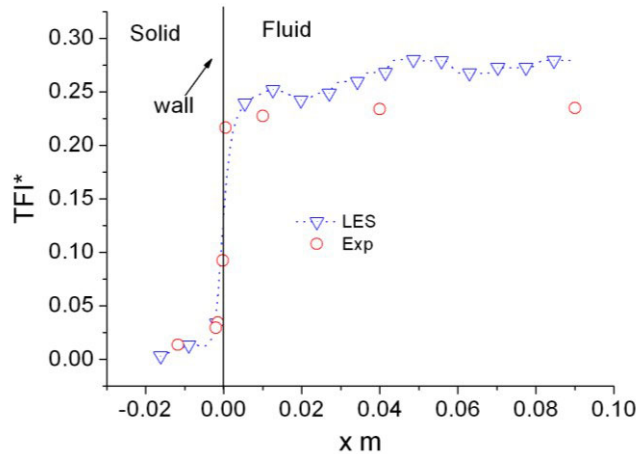


Figure 4-6. Temperature Fluctuation Intensity distribution in Normal Direction to Wall Surface

5. Conclusions

This paper presented the predictions of the PLAJECT experiment Case A1 with sodium coolant using STAR-CCM+. The influence of boundary conditions and conjugate heat transfer was studied. This investigation shows the issues related to employing symmetry boundary conditions, including the formation of asymmetric vortices that are non-physical. It also demonstrated the capability to employ an outlet boundary along the entire outer perimeter, e.g. both sides and the top, without inducing numerical instabilities. Employing conjugate heat transfer significantly improves the accuracy of predicting the temperature fluctuation intensity near the wall, but does not influence the predictions in the central plane significantly. The preliminary results of LES and URANS, with outlet boundaries and conjugate heat transferred, exhibited reasonably good agreement with experimental results for temperature fluctuation intensity, as well as the average temperature and vertical velocity components at the measurement locations.

Acknowledgement

The submitted manuscript has been created by UChicago Argonne, LLC, Operator of Argonne National Laboratory (“Argonne”). Argonne, a U.S. Department of Energy Office of Science laboratory, is operated under Contract No. DE-AC02-06CH11357. The U.S Government retains for itself, and others acting on its behalf, a paid-up nonexclusive, irrevocable worldwide license in said article to reproduce, prepare derivative works, distribute copies to the public, and perform publicly and display publicly, by or on behalf of the Government. Argonne National Laboratory’s work was supported by the US DOE Office of Nuclear Energy under contract number DE-AC02-06CH11357.

References

1. D. S. Wood, “Proposal for design against thermal striping”, *Nuclear Energy*, No.6, pp.433-437, 1980.
2. J. E. Brunings, “LMFBR thermal-striping evaluation”, Interim report, Research Project 1704-11, prepared by Rockwell International Energy Systems Group, EPRI-NP-2672, 1982.
3. C. Betts, C. Bourman and N. Sheriff, “Thermal striping in liquid metal cooled fast breeder reactors”, *NURETH-2*, Vol.2, pp.1292-1301, 1983.
4. S. Moriya, S. Ushijima, N. Tanaka, S. Adachi and I. Ohshima, “Prediction of Thermal Striping in Reactors”, *Int. Conf. Fast Reactors and Related Fuel Cycles*, Vol.1, pp.10.6.1-10.6.10, 1991.
5. A. Tokuhiro, N. Kimura, J. Kobayashi and H. Miyakoshi, “An investigation on convective mixing of two buoyant, quasi-planar jets with a non-buoyant jet in-between by ultrasound Doppler velocimetry”, *ICONE-6*, ICONE-6058, 1998.
6. D. Tenchine and H. Y. Nam, “Thermal hydraulics of co-axial sodium jets”, *Am. Inst. Chem. Engrs. Symp. Ser. 83*, No.257, pp.151-156, 1987.
7. D. Tenchine and J. P. Moro, “Experimental and numerical study of coaxial jets”, *NURETH-8*, Vol. 3, pp.1381-1387, 1997.
8. E. Merzari, “On the numerical simulation of thermal striping in the upper plenum of a fast reactor”, *ICAPP 2010*, San Diego, CA, USA, June 2010.
9. Lomperski, S. et al., 2012. PIV Accuracy and Extending the Field of View for Validation of Multi-Scale CFD Tools. In: *Advances in Thermal Hydraulics 2012 (ATH '12)*, San Diego, CA, USA, November.
10. A. Tokuhiro, N. Kimura and H. Miyakoshi, “An experimental investigation on thermal striping. Part I: Mixing of a vertical jet with two buoyant heated jets as measured by ultrasound Doppler velocimetry”, *NURETH-8*, Vol. 3, pp.1712-1723, 1997.
11. A. Tokuhiro and N. Kimura, “An experimental investigation on thermal striping. Mixing phenomena of a vertical non-buoyant jet with two adjacent buoyant jets as measured by ultrasound Doppler velocimetry”, *Nucl. Eng. Design*, 188, pp.49-73, 1999.

12. N. Kimura, A. Tokuhiko and H. Miyakoshi, "An experimental investigation on thermal striping. Part II: Heat transfer and temperature measurement results", NURETH-8, Vol. 3, pp.1724-1734, 1997.
13. N. Kimura, H. Kamide, P. Emonot and K. Nagasawa, "Study on Thermal Striping Phenomena in Triple-Parallel Jet - Investigation on Non-Stationary Heat Transfer Characteristics Based on Numerical Simulation -", NURETH-12, Log Number: 117, Pittsburgh, Pennsylvania, U.S.A. September 30-October 4, 2007.
14. N. Kimura, H. Miyakoshi and H. Kamide, "Experimental Investigation on Transfer Characteristics of Temperature Fluctuation from Liquid Sodium to Wall in Parallel Triple-jet", *Int. J. Heat and Mass Transfer*, 50, pp.2024-2036, 2007.
15. N. Kimura, H. Miyakoshi, H. Ogawa, H. Kamide, Y. Miyake and K. Nagasawa, "Study on Convective Mixing Phenomena in Parallel Triple-Jet along Wall - Comparison of Temperature Fluctuation Characteristics between Sodium and Water -", NURETH-11, Paper: 427, Avignon, France, October 2-6, 2005.
16. N. Kimura, H. Kamide, P. Emonot and K. Nagasawa, "Study on Thermal Striping Phenomena in Triple-Parallel Jet - Transfer Characteristics of Temperature Fluctuation in Sodium and Water based on Conjugated Numerical Simulation -", NUTHOS-7, Seoul, Korea, October 5-9, 2008.